

stressed that the attribution of the AS reaction to $T_2(n, \pi^*)$ rather than $T_1(\pi, \pi^*)$ cannot be made by way of CIDNP alone: it is based on both the CIDNP evidence for an AS via $\bar{R}\cdot\text{R}^{\cdot}$ ²³ and the earlier result that T_1 of **1a-c** undergoes the oxadi- π -methane rearrangement^{6,10a} but not the AS.

This reaction scheme is corroborated by fluorescence data. At 25 °C, in 3-methylpentane, the fluorescence quantum yield of **1a** is 3.6 times lower than that of **1c** ($\Phi_f = (9 \pm 3) \times 10^{-4}$), from which one may expect a similar ratio in singlet lifetimes for these ketones.²⁴ This significant difference in singlet lifetimes at 25 °C is in accord with the observed singlet CIDNP for **1a** and triplet CIDNP for **1c** at this temperature.

Our results unveil a novel aspect of β, γ -UK photochemistry and may provide a key to the understanding of the AS reaction. Studies on the temperature dependence of fluorescence²⁵ and product quantum yields are in progress to further quantify the present picture, and to rationalize the differences between **1a** and **1b, c**.

Acknowledgments. We thank Miss I. Gerlach and Dr. K. Hildenbrand for technical advice on the NMR spectrometer and Drs. Marlies and Manfred Mirbach for stimulating discussions.

References and Notes

- Presented in part at the GDCh Symposium on Photochemistry, Mülheim a. d. Ruhr, Nov 1978 (Symposium Abstract, p 49).
- For reviews, see the following: (a) Dauben, W. G.; Lodder, G.; Ipaktschi, J. *Top. Curr. Chem.* **1975**, *54*, 73–114. (b) Houk, K. N. *Chem. Rev.* **1976**, *76*, 1–74. (c) Schaffner, K. *Tetrahedron* **1976**, *32*, 641–653.
- Gonzenbach, H.-U.; Schaffner, K.; Blank, B.; Fischer, H. *Helv. Chim. Acta* **1973**, *56*, 1741–1752.
- Dalton, J. C.; Shen, M.; Snyder, J. J. *J. Am. Chem. Soc.* **1976**, *98*, 5023–5025.
- Schuster, D. I.; Eriksen, J.; Engel, P. S.; Schexnayder, M. S. *J. Am. Chem. Soc.* **1976**, *98*, 5025–5027.
- Mirbach, M. J.; Henne, A.; Schaffner, K. *J. Am. Chem. Soc.* **1978**, *100*, 7127–7128.
- Van der Weerd, A. J. A.; Cerfontain, H.; van der Ploeg, J. P. M.; den Hollander, J. A. *J. Chem. Soc., Perkin Trans. 2* **1978**, 155–160.
- Van der Weerd, A. J. A. Ph.D. Thesis, University of Utrecht, 1978.
- Baggiolini, E.; Schaffner, K.; Jeger, O. *Chem. Commun.* **1969**, 1103–1104.
- (a) Gonzenbach, H.-U.; Tegmo-Larsson, I.-M.; Grosclaude, J.-P.; Schaffner, K. *Helv. Chim. Acta* **1977**, *60*, 1091–1123. (b) Blank, B.; Fischer, H., unpublished work, as mentioned in ref 10a, footnote 7.
- Bruker WH90 spectrometer, light filter: 3 cm NiSO₄/CoSO₄ solution.¹² For other details, see Benn, R.; Dreeskamp, H. *Z. Phys. Chem. Neue Folge* **1976**, *101*, 11–23.
- Blank, B.; Henne, A.; Fischer, H. *Helv. Chim. Acta* **1974**, *57*, 920–936.
- CIDNP effects at 45 °C ($A =$ enhanced absorption, $E =$ net emission;¹⁴ see Figure 1): **1a**, A for signals a, c, and e, E for b and d; **2**, E for CH₃, A for CHO. Similar effects were observed in CD₃CN and C₆D₁₂ in the range 0–60 °C.
- Kaptein, R. *J. Am. Chem. Soc.* **1972**, *94*, 6251–6262.
- $g(\text{CH}_3\text{CO}) = 2.0005$, $a_H(\text{CH}_3\text{CO}) = +0.40$ mT.¹⁶ The following parameters were taken for the 1,2,3-trimethylcyclopentenyl radical R· ($X = Y = \text{CH}_3$) in analogy to similar allyl radicals:¹⁷ $g = 2.0026 \pm 0.0001$, $a_H(1\text{-and } 3\text{-CH}_3) = +1.5 \pm 0.15$ mT, $a_H(2\text{-CH}_3) = -0.32 \pm 0.02$ mT, $a_H(4\text{-and } 5\text{-CH}_2) = +2.1 \pm 0.2$ mT.
- Paul, H.; Fischer, H. *Helv. Chim. Acta* **1973**, *56*, 1575–1594. Bennet, J. E.; Mile, B. *Trans. Faraday Soc.* **1971**, *67*, 1587–1597.
- Berndt, H. "Landolt Börnstein, Magnetic Properties of Free Radicals", New Series, Vol. 9, Part b; Fischer, H., Hellwege, K.-H., Eds.; Springer: Berlin, 1977; pp 342–765.
- Variations in the relative CIDNP intensities with temperature (e.g., for **1a** vs. **2**) may well be induced by changes in the nuclear spin-relaxation times¹⁴ and disproportionation/combination ratios of the radical pair R·R'.¹⁹ However, this would not change the phases of the polarizations. In the low temperature experiments, biacetyl (**3**) can be unambiguously assigned. Its polarization is opposite to that of CH₃CHO, which is expected for a product derived from acetyl radicals that have escaped from the primary cage.¹⁴
- E.g., see the following: Gibian, M. J.; Corley, R. C. *Chem. Rev.* **1973**, *73*, 441–464. Schuh, H.; Fischer, H. *Int. J. Chem. Kinet.* **1976**, *8*, 341–356.
- Note that the intramolecular nature of the AS had been demonstrated for **1a** at room temperature only⁹ and that by analogy a similar AS mechanism for **1b** had been assumed.^{2c, 10a} In a previous, exploratory photo-CIDNP study of **1b**,^{10b} the strong influence of temperature on the magnitude of the polarization effects of the β, γ -UK had been ignored. The relatively weak effects observed were therefore believed to be insignificant mechanistically.
- Koenig, T.; Fischer, H. "Free Radicals", Vol. 1; Kochi, J. K., Ed.; Wiley-Interscience: New York, 1973; pp 157–189.
- Determined with $t_1(\text{CH}_3\text{CHO}) = 2.1$ s, using a small flip angle, $\alpha \sim 20^\circ$. See Schäublin, S.; Hohenner, A.; Ernst, R. R. *J. Magn. Reson.* **1974**, *13*, 196–216.
- CIDNP effects at -54 °C (for denotations see footnote 13 and Figure 2): **1c** and AS isomer, A for a, a', b, and (CH₂)₂ (δ 2.1–2.6), E for c, c', d, and d'. Effects with the same phase were observed in CD₃OD, CD₃CN, and C₆D₁₂ at temperatures ≤ 50 °C.
- This is a lower limit. Correction for the absorption coefficients of **1a** (λ_{max} 300 nm (ϵ_{max} 175)) and **1c** (λ_{max} 295 nm (ϵ_{max} 119)) increases the ratio of singlet lifetimes (τ_s) to

$$\frac{\tau_s(\mathbf{1c})}{\tau_s(\mathbf{1a})} = \left(\frac{\Phi_f(\mathbf{1c})}{\Phi_f(\mathbf{1a})} \right) \left(\frac{k_f(\mathbf{1a})}{k_f(\mathbf{1c})} \right) \approx \left(\frac{\Phi_f(\mathbf{1c})}{\Phi_f(\mathbf{1a})} \right) \left(\frac{\epsilon(\mathbf{1a})}{\epsilon(\mathbf{1c})} \right) \approx 5$$
- Preliminary results on the temperature-dependent luminescence of **1a** and **1c** strongly corroborate the present picture: Henne, A.; Hildenbrand, K.; Siew, N. P. Y.; Schaffner, K., unpublished work.

Andreas Henne, Nancy P. Y. Siew, Kurt Schaffner*

Institut für Strahlenchemie im
Max-Planck-Institut für Kohlenforschung
D-4330 Mülheim a. d. Ruhr, West Germany

Received January 9, 1979

Valence Electrons in Open-Shell Molecules: Experimental Studies Using Polarized Neutron Scattering

Sir:

Valence electron densities in crystals are being defined with increasing precision, very largely through the use of accurate X-ray diffraction measurements coupled to the neutron diffraction definition of nuclear positional and vibrational parameters (the X-N technique).¹ This method, although valuable, has limitations; for example, significantly accurate ($\sigma(\rho) \approx 0.01\text{--}0.02$ e Å⁻³) electron densities of the valence shells of transition metal complexes will remain difficult because of high local electron densities. An improvement in accuracy and interpretation can be achieved if the elastic scattering process could be referred exclusively to a relatively small number of the total electrons in the unit cell; this can be achieved via polarized neutron scattering experiments.

The electronic spin system of a paramagnetic single crystal can be ordered by the application of an external magnetic field (typically 1.5–5 T at 4.2 K) along the direction of polarization of the incident neutrons. For magnetic neutron scattering, only those magnetization components perpendicular to the scattering vector are effective. Therefore, only a limited three-dimensional set of magnetic structure factors is obtainable from any particular alignment of the crystal with respect to the applied magnetic field. Given $N(hkl)$ and $M(hkl)$ are the nuclear and magnetic structure factors, respectively; the observed Bragg intensities, $[N(hkl) \pm M(hkl)]^2$, result from coupling of the nuclear and magnetic scattering vectors. Precise magnetic structure factors can be obtained from "spin-flip" ratios,² $[N(hkl) + M(hkl)]^2/[N(hkl) - M(hkl)]^2$, of a large number of Bragg reflections whose nuclear structure factors have been determined from conventional diffraction experiments. Fourier inversion of the magnetic structure factors gives the magnetization density throughout the crystallographic unit cell, and maps of such densities have been described for simple ferro- and ferrimagnetic structures.³ In the absence of independent orbital angular momentum in the ground state of an ion, spin density may be directly related to magnetization density. We now outline the power of the method for transition metal compounds of chemical interest and complexity.

The five complexes to which we have access to extensive sets of magnetic structure factors are manganese- and cobalt-phthalocyanine, the hexafluorochromium(III) anion,⁴ the tetrachlorocobalt(II) anion, and aquabis(bipyridyl)di- μ -hydroxo-sulfatodicopper(II).

The magnetic structure factors may be analyzed quantitatively to provide local (atomic) spin densities and overlap charges in at least two ways. Firstly, the formulae for the

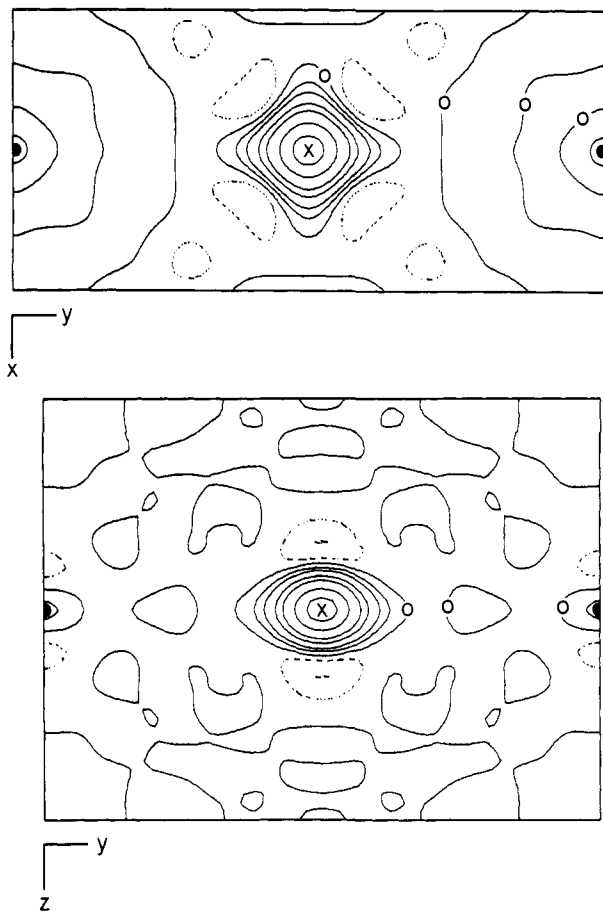


Figure 1. Fourier sections of the Cs_3CoCl_5 magnetic data. Cobalt and cesium atoms are indicated by crosses and filled circles, respectively. The magnetization density was averaged over a cube of 0.1 \AA dimensions. The contours are at intervals of 0.7, 0.5, 0.3, 0.2, 0.1, 0.05, 0, -0.05 , and $-0.10 \mu_B \text{ \AA}^{-3}$, and some important zero contours are indicated. Negative areas, enclosed by dotted contours, represent magnetization of reverse polarity to the bulk moment.

scattering by nonspherical d- and p-electron distributions,⁵ together with the relevant orbital scattering factors (from either a tabulated source⁶ or calculated from the Hartree-Fock wave functions⁷), can be used in a least-squares refinement of the ground-state spin populations of the one-center atomic orbital expansions. This has been done for the 69 observed magnetic structure factors⁴ for $\text{K}_2\text{Na}(\text{CrF}_6)$ having values $M(hkl) \geq 2\sigma[M(hkl)]$. Refinement analysis minimizing the function $\sum w(\Delta M)^2$ where $\Delta M = |M_o| - |M_c|$ and $w = 1/\sigma^2[M(hkl)]$ gives the d-orbital populations on the chromium atom, $d_{x^2-y^2}$ 0.87(2), d_{xz} 0.87(2), d_{yz} 0.87(2), d_{z^2} 0.00(3), $d_{x^2-z^2}$ 0.00(3), and 0.11 (3) e in a spherically symmetric s-type function on each fluorine atom. That the sum of the spin density on each $(\text{CrF}_6)^{3-}$ complex is not identical with three electrons results from our neglect, as yet, of spin density in the overlap regions which is apparent in observed⁴ and difference spin density Fourier syntheses. For this atom spin density scattering model, the residual index R , defined as $\sum |\Delta M| / \sum |M_o|$, is 0.096 and the goodness of fit (χ), defined as $[\sum w(\Delta M)^2 / (n - v)]^{1/2}$ where n is the number of observations and v is the number of variables, is 1.79. For the corresponding spherical model (i.e., the same orbital populations but ignoring the aspherical terms in the scattering formulae), the agreement factors are $R = 0.187$ and $\chi = 3.46$. A refinement based on a purely ionic model alone (i.e., with no spin density delocalized onto the fluorine) gives $R = 0.102$ and $\chi = 1.97$, reinforcing intuition to the extent that a purely ionic model gives, for $(\text{CrF}_6)^{3-}$, a very fair quantitative account of the magnetic scattering. The t_{2g} orbital occupation expected on the basis of ligand field

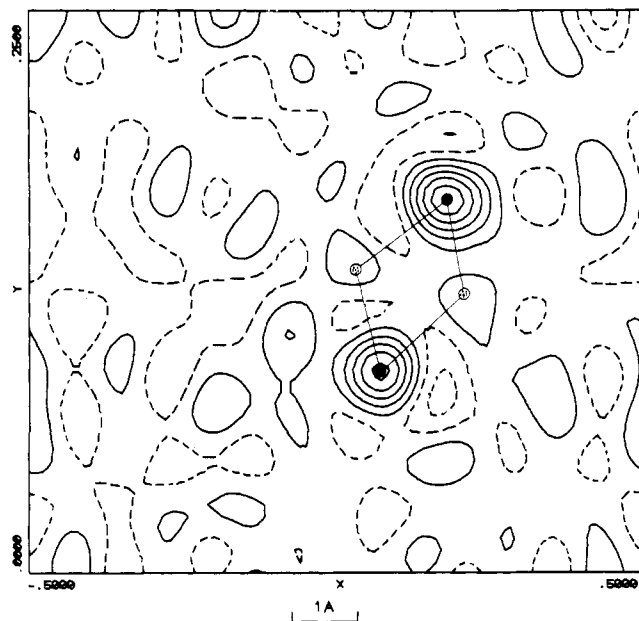
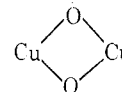


Figure 2. Section perpendicular to $[001]$ of the observed spin density distribution from 110 reflections with $\sin \theta / \lambda \leq 0.4 \text{ \AA}^{-1}$ for aquabis(bipyridyl)di- μ -hydroxo-sulfatodicopper(II). The



core is indicated with solid and dotted circles representing Cu and O, respectively. The density was averaged over a cube of 0.5 \AA dimensions. Contours are at intervals of 0.45, 0.35, 0.25, 0.15, 0.05, -0.05 , and $-0.15 \mu_B \text{ \AA}^{-3}$.

theory is well supported and spin transfer $\text{Cr} \rightarrow \text{F}$ is demonstrated to the same extent as deduced previously.⁴ In the refinements, the value of $M(000)$ obtained from the bulk magnetization measurement⁴ was used to scale the calculated magnetic structure factors, scattering curves were for $\text{Cr}^{3+}(3d)$ and $\text{F}(2p)$,⁶ and atomic positional and thermal parameters were taken from the 4.2 K nuclear structure determination.⁴

Nuclear and magnetic structure factors have been determined from single crystals of Cs_3CoCl_5 at 4.2 K; magnetic,⁸ structural,⁹ and theoretical data¹⁰ on the $(\text{CoCl}_4)^{2-}$ ion have been reported previously. Fourier inversion of the 124 magnetic structure factors having $M(hkl) \geq 2\sigma[M(hkl)]$ is shown in Figure 1 and demonstrates the asphericity of the magnetization density about the cobalt atom. Again, a quantitative analysis of the structure factors has been completed; the least-squares analysis gives $d_{x^2-y^2}$ 0.36(13), d_{xz} 0.85(6), d_{yz} 0.85(6), d_{z^2} $-0.10(11)$, $d_{x^2-z^2}$ 0.53(15) on the cobalt atom, p_x $-0.05(3)$, p_y 0.04(1), p_z 0.13(2) on the chlorine ligand (where p_x is along the Cl-Co bond), and -0.04 (2) e in a spherical s-type "blob" in the Co-Cl overlap region. For all 154 observed magnetic structure factors, refinement converged to give $R = 0.102$ and $\chi = 3.13$ using $M(000)$ ⁸ to scale M_c , scattering curves for $\text{Co}^{2+}(3d)$ ⁶ and $\text{Cl}(3p)$,⁷ and atomic positional and thermal parameters from the 4.2 K nuclear structure determination.¹¹ The dipole approximation¹² with $g = 2.3$ was used to correct for the orbital contribution to the magnetic structure factors. Here, the t_{2g} orbital occupation expected on the basis of ligand field theory is not found. It appears that spin has been transferred from the d_{xy} orbital (the x - y - z coordinate system corresponds to the crystal axes) to the $d_{x^2-y^2}$ orbital which, interestingly, is directed toward cesium ions.

The second quantitative approach is useful for the more covalent complexes for which the ionic model provides a less adequate representation of the magnetic structure factors. We are developing computer programs which analyze spin densities

via localized atomic deformation functions;¹³ these can, in favorable cases, be handled to give a conventional orbital description. For the phthalocyanine complexes, the Fourier series indicates a total delocalization of spin density onto the ligand of >20%, and we shall discuss these results in detail elsewhere.¹³

For the binuclear copper(II) complex, the copper atoms interact ferromagnetically with an exchange integral of 24 cm^{-1} ; the observed density distribution shows no significant spin density between the copper atoms (Figure 2), whereas spin density is present on the bridging hydroxyl ligands, and this indicates that the mechanism of magnetic coupling is essentially one of superexchange.

Note Added in Proof. Further analysis of the data for Cs_3CoCl_5 to include refinement of the cobalt scattering curve shape and consideration of the bias introduced into the Fourier maps by an incomplete data set has led to d-orbital populations on the cobalt closer to the expected t_3^3 .

Acknowledgments. We are grateful to the S.R.C. for support. B.N.F. acknowledges sabbatical leave from the University of Western Australia and G.A.W. thanks the University of Melbourne for a Travelling Scholarship. We are most grateful to Drs. P. J. Brown and J. B. Forsyth for very helpful discussions. The neutron-diffraction data were obtained at the I.L.L., Grenoble.

References and Notes

- (1) For example, the review papers in *Isr. J. Chem.*, **16**, 87-229 (1977).
- (2) B. C. Tofield, *Struct. Bonding (Berlin)*, **21**, 1 (1975).
- (3) For example, R. S. Perkins and P. J. Brown, *J. Phys. F*, **4**, 906 (1974).
- (4) F. A. Wedgwood, *Proc. R. Soc. London, Ser. A*, **349**, 447 (1976).
- (5) R. J. Weiss and A. J. Freeman, *J. Phys. Chem. Solids*, **10**, 147 (1959).
- (6) "International Tables for X-ray Crystallography", Vol. 4, Kynoch Press, Birmingham, 1974, pp 103-146.
- (7) E. Clementi and C. Roetti, *At. Data Nucl. Data Tables*, **14**, 177 (1974).
- (8) B. N. Figgis, M. Gerloch, and R. Mason, *Proc. R. Soc. London, Ser. A*, **279**, 210 (1964); R. P. van Staple, H. G. Beljers, P. F. Bongers, and H. Zijlstra, *J. Chem. Phys.*, **44**, 3719 (1966); K. W. Mess, E. Lagendijk, D. A. Curtis, and W. J. Huiskamp, *Physica*, **34**, 126 (1967).
- (9) B. N. Figgis, M. Gerloch, and R. Mason, *Acta Crystallogr.*, **17**, 506 (1964).
- (10) I. H. Hillier, J. Kendrick, F. E. Mabbs, and C. D. Garner, *J. Am. Chem. Soc.*, **98**, 395 (1976).
- (11) B. N. Figgis, R. Mason, A. R. P. Smith, and G. A. Williams, submitted to *Acta Crystallogr.*
- (12) W. Marshall and S. W. Lovesey, "Theory of Thermal Neutron Scattering", Clarendon Press, Oxford, 1971, p 152.
- (13) B. N. Figgis, L. Leiserowitz, R. Mason, P. A. Reynolds, A. R. P. Smith, J. N. Varghese, and G. A. Williams, unpublished work.
- (14) V. H. Crawford, H. W. Richardson, J. R. Wasson, D. J. Hodgson, and W. E. Hatfield, *Inorg. Chem.*, **15**, 2107 (1976).
- (15) Authors to whom correspondence should be sent at the following address: School of Chemistry, University of Western Australia, Nedlands, 6009, Western Australia.

Brian N. Figgis*¹⁵

School of Chemistry, University of Western Australia
Nedlands, 6009, Western Australia

Ronald Mason, Andrew R. P. Smith, Geoffrey A. Williams*¹⁵

School of Molecular Sciences, University of Sussex
Brighton BN1 9QJ, United Kingdom

Received November 27, 1978

Photochemical Probes for Model Membrane Structures

Sir:

We have described the selective attack of benzophenone probes on rigid steroids¹ and the more random attack on flexible chains. The latter, useful chiefly as evidence on conformations of the chain, was examined in homogeneous solution² and in micelles.³ We concluded that a probe such as benzophenone-4-carboxylate (**2**) incorporates into a micelle

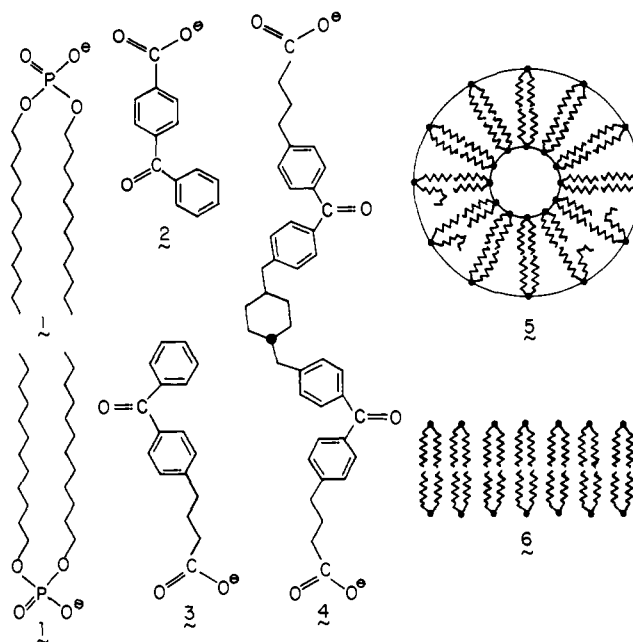


Figure 1. Probes and bilayers.

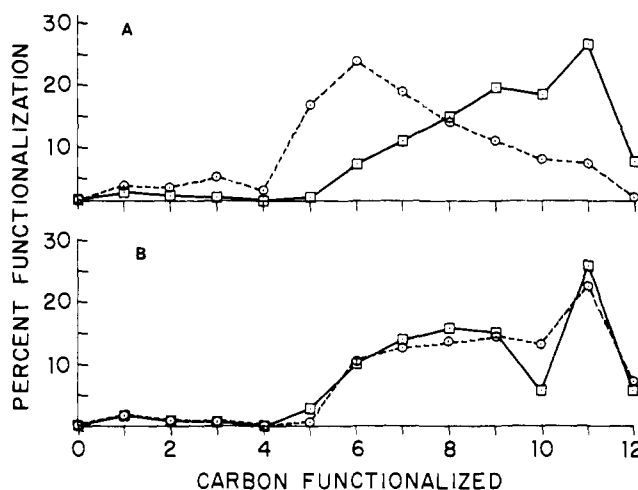


Figure 2. Distribution of functionalized positions. A: probe 2 with bilayer 1 as a vesicle (□) and as a multilamellar system (○). B: vesicles of 1 with probe 3 (□) and probe 4 (○).

such as that from sodium dodecyl sulfate (SDS) so that the probe orients largely perpendicular to the micelle surface. However, on photoexcitation it attacks a range of the CH_2 's of SDS because of the disorder of the SDS chains.

Amphiphiles with two chains per charged head group, such as didodecyltrimethylammonium cation,⁴ dicetylphosphate anion,⁵ and the lecithin of biomembranes⁶ tend to form bilayers, not micelles, in which the chains are presumably more ordered than those in simple micelles. Such bilayers can exist as flat sheets, as in multilamellar structures, or instead as the curved surface of a spherical vesicle.⁶ NMR evidence has been interpreted⁷ to indicate that the bilayers of small spherical vesicles are more disordered than are the bilayers of multilamellar structures, although this interpretation has been disputed.⁸ Thus it was of interest to apply our benzophenone probe method to the study of bilayers.⁹ With this technique we have been able to explore the amount of disorder in such structures, and to demonstrate a striking difference between the disorder in spherical vesicles (**5**) and that in flat multilamellar systems (**6**) (Figure 1).

Our bilayers were constructed from didodecyl phosphate (**1**).¹⁰ When this was sonicated¹¹ at 16 mM with 8 mM **2** in 50 mM Tris buffer at pH 8.0, a clear stable solution was formed